

## STRUCTURE OF ODD-ODD In NUCLEI

TIBOR FÉNYES, ZSOLT DOMBRÁDI, ATTILA KRASZNAHORKAY, JÁNOS GULYÁS,  
JÁNOS TIMÁR and TIBOR KIBÉDI

*Institute of Nuclear Research of the Hung. Acad. Sci., 4001 Debrecen, Hungary  
and*

VLADIMIR PAAR

*Prirodoslovno-matematički fakultet, University of Zagreb, 41000 Zagreb, Yugoslavia*

Received 25. July 1989

UDC 539.144

Original scientific paper

The structure of  $^{114,112,110,108,106}\text{In}$  nuclei was studied with complex  $\gamma$  and electron spectroscopic methods via  $(p, n\gamma)$  and (in cases of  $^{112,110}\text{In}$ )  $(\alpha, n\gamma)$  reactions at 4.8—17.1 MeV bombarding particle energies. New level schemes have been deduced. The energy splitting of proton-neutron multiplet states of  $^{116,114,112,110,108,106}\text{In}$  was calculated on the basis of the »parabolic rule«, and the results have been compared with the existing experimental data. The energy spectra and electromagnetic properties of odd-odd  $^{116-106}\text{In}$  nuclei were calculated in the framework of the interacting boson-fermion-fermion/odd-odd truncated quadrupole phonon model (IBFFM/OTQM). The main systematic trends and changes in nuclear structure have been reasonably well described by the theory.

### *1. Introduction. Experimental methods and results*

In the last few years a large amount of experimental information has been obtained on the odd-odd In nuclei providing a reliable basis for theoretical analysis.

The excited states of odd-odd In nuclei have been studied in beams of the Debrecen 103 cm and Jyväskylä 90 cm isochronous cyclotrons via  $(p, n\gamma)$  and  $(\alpha, n\gamma)$  reactions. The targets were prepared from enriched Cd and Ag isotopes.

The nuclear spectroscopic channels of the Debrecen cyclotron and the experimental facilities are shown in Fig. 1. On the  $\gamma(-e^-)$  channel a turning table was installed for supporting various semiconductor detectors. Replaceable reaction

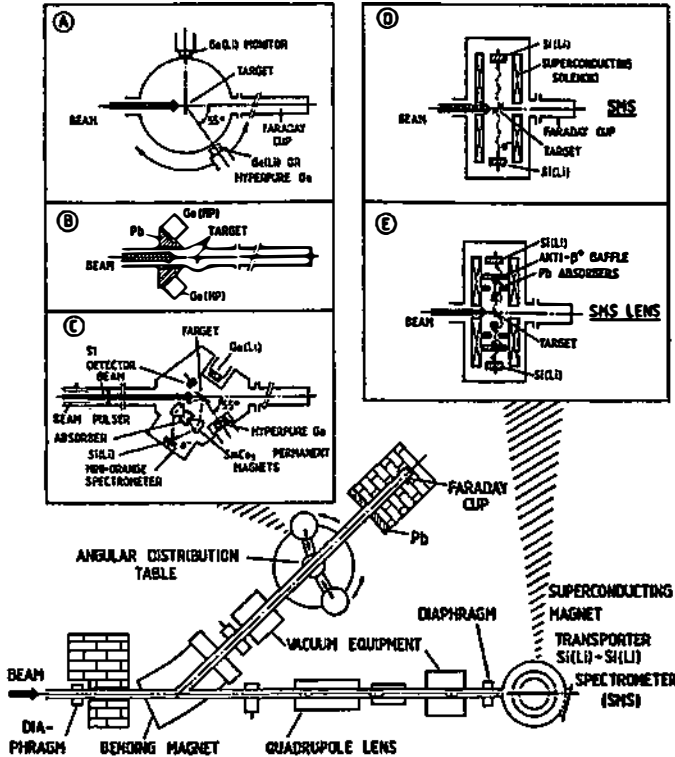


Fig. 1. Layout of the  $\gamma$ - and electron-spectroscopic beam channels of the Debrecen 103 cm cyclotron; reaction chambers, spectrometers and types of measurements. SMS: superconducting magnet transporter Si (Li)-Si (Li) electron spectrometer.

chambers (A-C) provide possibility for single  $\gamma$  spectrum,  $\gamma$ -ray angular distribution, different coincidence, and lifetime measurements. For conversion electron studies a minorange Si (Li) spectrometer was used in the chamber C.

On the electron spectroscopic channel a superconducting magnet transporter Si (Li)-Si (Li) spectrometer (SMS) was installed, which could be operated both without and with central absorber [in the latter case as a lens spectrometer (SMLS)].

In order to obtain »complete« spectroscopic information on odd-odd indium nuclei  $\gamma$ -ray spectra ( $E_\gamma$ ,  $I_\gamma$ ),  $\gamma\gamma$  coincidences, internal conversion electron spectra,  $\gamma$ -ray angular distributions, lifetimes of excited levels (by means of Doppler-shift and delayed coincidence methods), and relative reaction cross sections [ $\sigma_{rel}(E_{LEV})$ ] were measured at different bombarding particle energies. Level schemes, level energies ( $E_{LEV}$ ), spins, parities,  $\gamma$ -branching ratios and  $\gamma$ -mixing ratios have been deduced.

The experimental results were published in detail in the following papers:  $^{114}\text{In}^1)$ ,  $^{112}\text{In}^2)$ ,  $^{110}\text{In}^{3,4)}$ ,  $^{108}\text{In}^5)$  and  $^{106}\text{In}^6)$ . The low-energy parts of level schemes of odd-odd  $^{116-106}\text{In}$  nuclei are shown in Figs. 2—4 (columns d).

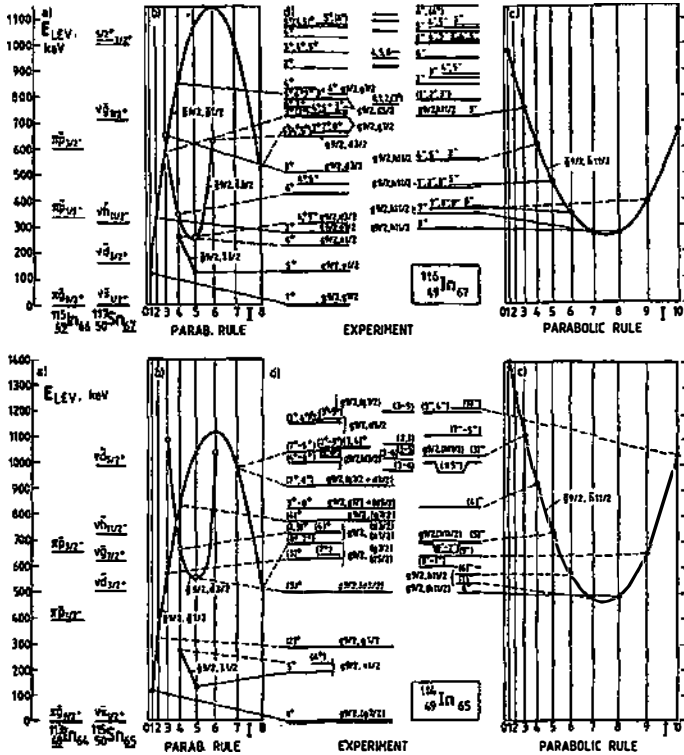


Fig. 2. Up: Level scheme and p-n multiplet states of  $^{116}\text{In}$ . a) Experimental level energies ( $E_{LEV}$ ) and main configurations of the low-lying states of  $^{115}\text{In}$  and  $^{117}\text{Sn}$ . b) and c) Results of parabolic rule calculations, separately for positive and negative parity levels. On the abscissa  $I(I + 1)$  is shown, where  $I$  is the spin of the state.

d) Experimental results on  $^{116}\text{In}$  levels<sup>7)</sup>.  
Down: Level scheme and p-n multiple states of  $^{114}\text{In}^{11)$ .

## 2. Proton-neutron multiplet states and the parabolic rule

In zeroth order approximation the level energies of odd-odd nuclei can be obtained by addition of energies of the odd proton and odd neutron states. In higher order approximations the proton-neutron residual interaction must be taken into account, too. If we consider the residual interaction as a consequence of quadrupole and spin vibrational phonon exchanges between proton and neutron through the nuclear core, a «parabolic rule» can be deduced from the cluster-vibration model (Paar<sup>8)</sup>). By the use of the parabolic rule the energy splitting of proton-neutron multiplet states (as a function of the nuclear spin ( $I$ )) was successfully described in many cases<sup>8,9,10)</sup>. Near closed proton and neutron shells (or

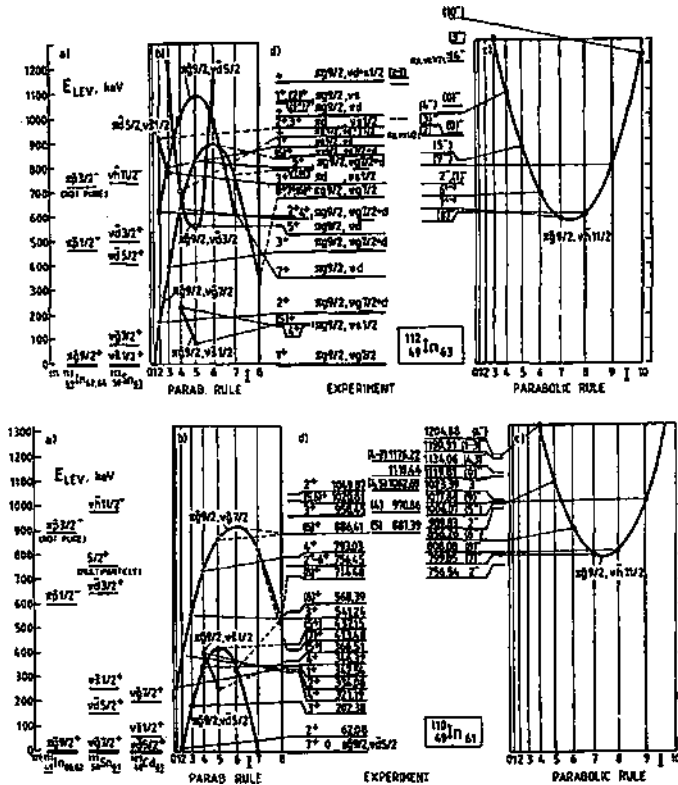


Fig. 3. Level schemes and p-n multiplet states of  $^{112}\text{In}^2$  (up) and  $^{110}\text{In}^{3,4}$  (down). Further explanations see under Fig. 2 and in text.

subshells) some minor deviations were observed from the predictions of the rule (see Ref. 9 for the case of  $^{92}\text{Nb}_{51}$  and  $^{96}\text{Nb}_{55}$ ). In the present work we have studied the applicability of the parabolic rule in a wide region of In nuclei from  $A = 116$  to 106.

### 2.1. Basic formulae

The low-lying levels of odd-odd nuclei can be described in leading order approximation by the following formulas<sup>8)</sup> assuming quadrupole-quadrupole and spin-spin residual interactions

$$E(I) = E_{j_p} + E_{j_n} + \delta E_2 + \delta E_1, \tag{1}$$

$$\delta E_2 = -a_2 \mathcal{V}.$$

$$\mathcal{V} = \frac{[I(I+1) - j_p(j_p+1) - j_n(j_n+1)]^2 + I(I+1) - j_p(j_p+1) - j_n(j_n+1)}{2j_p(2j_p+2)2j_n(2j_n+2)} + \mathcal{V} \frac{a_2}{12}, \tag{2}$$

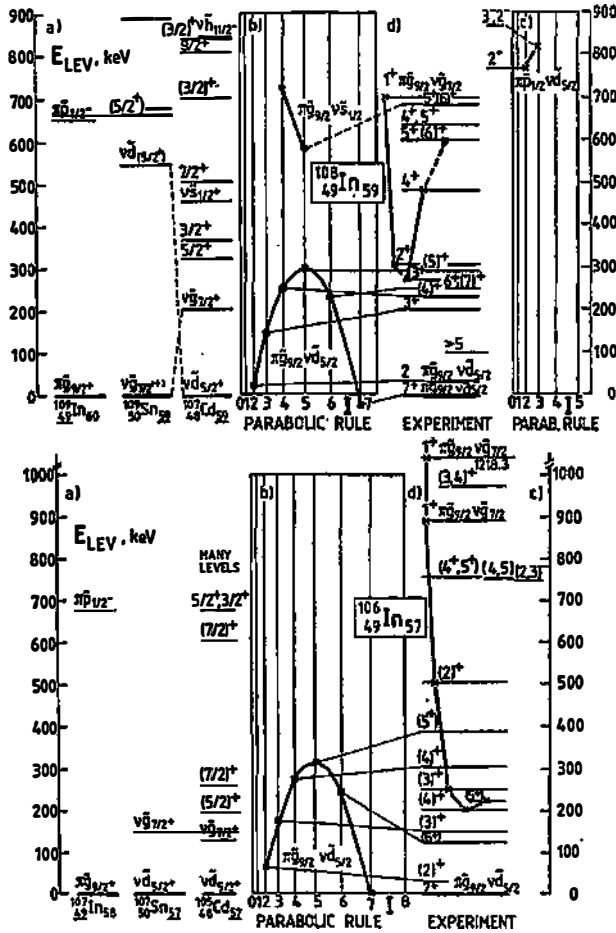


Fig. 4. Level schemes and p-n multiplet states of  $^{108}\text{In}^5$  (up) and  $^{106}\text{In}^6$  (down). Further explanations see under Fig. 2 and in text.

$$\delta E_1 = -\alpha_1 \xi \frac{I(I+1) - j_p(j_p+1) - j_n(j_n+1)}{(2j_p+2)(2j_n+2)}. \quad (3)$$

Here  $E(I)$  is the energy of the level,  $E_{j_p}$  and  $E_{j_n}$  denote the quasiproton and quasineutron energies, respectively,  $I = |j_p - j_n|, \dots, j_p + j_n$ , where  $j$  is the total angular momentum of the quasiparticle.  $\delta E_2$  and  $\delta E_1$  describe the energy splitting of the proton-neutron multiplet as a consequence of the quadrupole and dipole interactions between (quasi)proton and (quasi)neutron through the nuclear core.  $\alpha_2$  and  $\alpha_1$  are the quadrupole and dipole force strengths, respectively. The definitions of  $\mathcal{V}$  and  $\xi$  coefficients are given in Ref. 8.

The dependence of the coupling strengths on the occupation probability of levels may be described by the following approximate formulas<sup>8)</sup>

$$a_2(j_p, j_n) = \alpha_2^{(0)} |(U_{j_p}^2 - V_{j_p}^2)(U_{j_n}^2 - V_{j_n}^2)|,$$

$$a_1(j_p, j_n) = \alpha_1^{(0)},$$

where  $V_j^2$  is the probability of occupation of the level  $j$  and  $U^2 = 1 - V^2$ .

The extension of formulae (2)–(3) on proton-phonon-neutron, as well as on cluster states is given in Ref. 11.

The parabolic rule can be realized also in Bose-Fermi symmetry schemes<sup>12)</sup>, if we make an algebraic distinction between the fermion representations which are primarily particle-like and those which are primarily hole-like. This realization is a consequence of the group structure.

## 2.2. Parameters

The quasiparticle energies were taken from the experimental data of the neighbouring single-odd nuclei. Nevertheless in practice a separate energy normalization was needed at each p-n multiplet on the basis of one (or more) realibly identified state(s) of the odd-odd nucleus. This normalization pushed up (or down) all members of the multiplet, without changing the shape of the energy splitting.

The  $\alpha_1^{(0)}$ ,  $\alpha_2^{(0)}$  and  $V^2$  parameters used in the calculations are summarized in Table 1.

The  $\alpha_1^{(0)}$  values were calculated from the expression  $\alpha_1^{(0)} \approx 15/A$  MeV, where  $A$  is the mass number.

$\alpha_2^{(0)}$  may be estimated from the data of neighbouring even-even nuclei, on the basis of the formula  $\alpha_2^{(0)} = 382 \beta_2^2 (\hbar\omega_2)^{-1}$  MeV (natural parametrization), where  $\hbar\omega_2$  is the energy of the first  $2^+$  state (in MeV) and  $\beta_2$  is the quadrupole deformation parameter. Nevertheless phenomenological  $\alpha_2^{(0)}$  values, obtained from fitting the parabola to experimental data, gave better results.

The occupation probabilities of the quasiparticle states were taken from the systematics of the experimental data.

## 2.3. Results

The experimental and theoretical level schemes of <sup>116,114,112,110,108,106</sup>In are shown in Figs. 2–4.

In columns a) the low-lying levels of the neighbouring single-odd nuclei are given, as well as the main components of the wave functions of the states. The configurations were deduced mainly from one-nucleon transfer reaction studies.

Columns b) and c) show the results of parabolic rule calculations, separately for positive and negative parity states.

In columns d) the experimental level schemes are given, as well as the main components of the wave functions, obtained mostly from one-nucleon transfer reaction studies.

The members of proton-neutron multiplets have been identified on the basis of experimental level energies, spins, parities, known electromagnetic moments,  $l_n$ ,  $l_p$  values of one-nucleon transfer experiments and the electromagnetic decay properties of the levels (multipolarities of transitions and reduced branching ratios<sup>3)</sup>). It is known that between neighbouring  $I \rightarrow (I \pm 1)$  states of the same proton-neutron multiplet one can expect strong  $M1$  transitions.

TABLE 1.

Isotope	$\alpha_1^{(0)}$ , MeV*	$\alpha_2^{(0)}$ , MeV		$V^{2***}$				
		fitted to exp. data	from natural parametrization**	$\pi g_{9/2}$	$\nu d_{5/2}$	$\nu g_{7/2}$	$\nu d_{3/2}$	$\nu h_{11/2}$
$^{116}_{49}\text{In}_{67}$	0.13	8.7	$^{116}\text{Sn}$ : 3.8 $^{118}\text{Sn}$ : 4.2 $^{116}\text{Cd}$ : 30.1	0.87		0.82	0.30	0.29
$^{114}_{49}\text{In}_{65}$	0.13	8.7	$^{114}\text{Sn}$ : 4.1 $^{116}\text{Sn}$ : 3.8 $^{114}\text{Cd}$ : 25.5	0.87	0.70	0.82	0.23	0.22
$^{112}_{49}\text{In}_{63}$	0.13	8.7	$^{112}\text{Sn}$ : 5.1 $^{114}\text{Sn}$ : 4.1 $^{112}\text{Cd}$ : 21.4	0.87	0.70	0.78	0.17	0.18
$^{110}_{49}\text{In}_{61}$	0.13	8.7	$^{110}\text{Sn}$ : 7.1 $^{112}\text{Sn}$ : 5.1 $^{110}\text{Cd}$ : 19.4	0.87	0.68	0.70		0.17
$^{108}_{49}\text{In}_{59}$	0.13	8.7	$^{108}\text{Sn}$ : 6.2 $^{110}\text{Sn}$ : 7.1 $^{108}\text{Cd}$ : 22.9	0.87	0.63			
$^{106}_{49}\text{In}_{57}$	0.14	8.7	$^{106}\text{Sn}$ : 5.8 $^{108}\text{Sn}$ : 6.2 $^{106}\text{Cd}$ : 20.9	0.87	0.62			

Parameters used in the parabolic rule calculations.

## 2.4. Conclusions

A) More than 80 p-n multiplet states\* have been identified in  $^{116,114,112,110,108,106}\text{In}$ . In all cases the calculations correctly reproduced the type of parabola (i. e. open up or down). The minimum energy members of multiplets were also correctly predicted. (The special W-like splitting of the  $\pi g_{9/2} \nu g_{7/2}$  multiplet in  $^{110,108}\text{In}$  will be discussed in Chapter 3.)

B) Using the same  $\alpha_1^{(0)} \approx 0.13$  MeV and  $\alpha_2^{(0)} = 8.7$  MeV interaction strengths for all multiplets the energy of more than 80 multiplet states could be described with  $\approx 80$  keV rms deviation (after the normalization shifts). The  $\alpha_1^{(0)}$  parameter, obtained from fitting to measured data, is not far from the values predicted by «natural parametrization» (Table 1).

\*  $\alpha_1^{(0)} = \alpha_1 \approx 15/A$  MeV.

\*\* Calculated from experimental  $\beta_2$  and  $E(2^+) = \hbar\omega_2$  MeV data on the basis of the formula  $\alpha_2^{(0)} = 382 \beta_2^2 / \hbar\omega_2$  MeV.

\*\*\* Obtained from the systematics of experimental and theoretical data on the basis of about 30 publications (see <sup>35,39,41-45,11</sup> etc.) in Ref. 3).

\* This number does not include the members of the  $\pi g_{9/2} \nu g_{7/2}$  multiplet of  $^{110,108,106}\text{In}$ .

The discrepancies may be due to different sources: configuration mixing of states, neglect of higher order terms and additional correlations, uncertainties of experimental data, non optimal procedure for determining parameters, etc.

C)  $\alpha_1^{(0)}/\alpha_2^{(0)}$  is less than 0.02 for the identified p-n multiplet states of  $^{116,114,112,110,108,106}\text{In}$ . This indicates that the influence of the dipole interaction compared with the quadrupole one is weak.

D) Smooth parabolas have been obtained for example at the  $\pi\tilde{g}_{9/2}\nu\tilde{h}_{11/2}$  multiplet of  $^{116,114,112,110}\text{In}$ . These nuclei are far from closed neutron shells, and the energy splitting of the multiplet is produced mainly by the quadrupole interaction.

Near double magic numbers (or subshell closures), where the core polarization interaction is not strong, the short-range interactions may play more important role. A definite energy staggering was observed for example in the case of the  $\pi\tilde{g}_{9/2}\nu\tilde{d}_{5/2}$  multiplet of  $^{106}\text{In}_{57}$ , similar to  $^{92}\text{Nb}_{51}$  and  $^{96}\text{Nb}_{55}$ <sup>9)</sup> ( $Z = 40$  and  $N = 56$  are semimagic numbers in  $_{40}\text{Zr}$  isotopes).

E) Worth mentioning that the ground states in  $^{116}\text{In}_{67}$ ,  $^{114}\text{In}_{65}$  and  $^{112}\text{In}_{63}$  are the  $J = 1^+$  members of the  $\pi\tilde{g}_{9/2}\nu\tilde{g}_{7/2}$  multiplet, although in the neighbouring  $^{117}\text{Sn}_{67}$ ,  $^{115}\text{Sn}_{65}$  and  $^{113}\text{Sn}_{63}$  nuclei the  $\nu\tilde{g}_{7/2}$  states have relatively high energy (712, 613 and 77 keV, respectively). In the case of opposite  $j_p$  and  $j_n$  alignment there is a strong overlap between the  $5\tilde{g}_{9/2}$  proton and  $5\tilde{g}_{7/2}$  neutron wave functions (spin-orbit partner states), consequently the proton-neutron interaction will be strong, and the  $1^+$  states sink down.

F) The energy splitting of the  $\pi\tilde{g}_{9/2}\nu\tilde{g}_{7/2}$  multiplet has an open-down parabolic form in  $^{116,114,112}\text{In}$  and a (distorted) open-up form in  $^{116}\text{In}$ . This inversion can be understood on the basis of the parabolic rule, because the quasi-neutron has a hole-like character in  $^{116,114,112}\text{In}$  and a particle-like in  $^{106}\text{In}$  (sign change in the  $(U^2 - V^2)$  factor). The distortion of the parabolic shape of the  $\pi\tilde{g}_{9/2}\nu\tilde{g}_{7/2}$  multiplet in  $^{110,108}\text{In}$  (and partly in  $^{106}\text{In}$ ) can be interpreted in IBFFM/OTQM (Chapter 3).

### 3. IBFFM/OTQM calculations

In order to get a deeper insight into the structure of odd-odd In nuclei, a detailed calculation of the energy spectra and electromagnetic properties of  $^{116,114,112,110,108,106}\text{In}$  nuclei was performed in the framework of IBFFM/OTQM. Besides level energies, spins and parities these calculations give information also on the wave functions, nuclear moments and reduced transition probabilities. IBFFM and OTQM are equivalent models at a phenomenological level<sup>1,2)</sup>. In the following we use the OTQM representation.

#### 3.1. Hamiltonian

The hamiltonian of the OTQM<sup>11)</sup> is given by

$$H_{OTQM} = H_{TQM} + \sum_{i=p,n} H^i + \sum_{i=p,n} H_{p\nu i} + H_{RES}$$

where  $H_{TQM}$  is the  $SU(6)$  quadrupole phonon hamiltonian of the even-even core.

$H^i$  denotes the quasiparticle hamiltonian of the odd proton ( $i = p$ ) and odd neutron ( $i = n$ ) in a spherical potential.

$H_{PVI}^i$  is the hamiltonian of the particle-vibration interaction for proton and neutron, which consists of three terms<sup>1,3)</sup>:

$$H_{PVI}^i = H_{MON}^i + H_{DYN}^i + H_{EXC}^i.$$

Here  $H_{MON}^i$  is the hamiltonian of the monopole interaction, which is proportional to the  $A_0^i$  monopole interaction strength.  $H_{DYN}^i$  characterizes the dynamical interaction (proportional to the  $I_0^i$  strength).  $H_{EXC}^i$  denotes the hamiltonian of the exchange interaction (with  $A_0^i$  strength).

$H_{RES}$  is the residual interaction between the odd proton and neutron. We have considered only a central delta force of the form  $H_{RES} = 4\pi\delta(\vec{r}_p - \vec{r}_n)[v_D + v_S\sigma_p\sigma_n]$ , where  $v_D$  and  $v_S$  are the parameters of the Wigner and Bartlett forces,  $\delta$  is the Dirac  $\delta$  symbol,  $\vec{r}_p$  and  $\vec{r}_n$  are the position vectors of the proton and neutron, respectively and the  $\sigma$ -s are the Pauli spin matrices.

The hamiltonian was diagonalized in the quasiproton-quasineutron weak coupling basis  $(j_p j_n) I, NR; J$ , where  $I$  is the resulting angular momentum of the  $j_p$  and  $j_n$  states,  $R$  is the angular momentum of the  $N$ -phonon state, and  $J$  is the total angular momentum.

The computer code IBFFM/OTQM used in the calculation was written by Brant, Paar and Vretenar<sup>1,4)</sup> and adopted for the Debrecen computers by Zs. Dombrádi.

### 3.2. Parametrization

The parameters used in the calculations are summarized in Table 2.

The core excitations were approximated with harmonic (or near harmonic) vibration. This is an acceptable approach, if we want to describe only low energy states, where the contribution of two and higher phonon components is small. We used the energies of the  $2_1^+$  states of the neighbouring even-even Sn nuclei as effective phonon energies ( $\hbar\omega_2$ ).

Since we are considering the low-lying states in the nearly spherical nuclei we can use reduced boson/phonon number,  $N_{max} = 2^{1,2)}$ . This strongly reduces the scope of computations, without a sizeable effect on the properties of the low-lying states which are being investigated. In some cases we have performed test calculations with  $N_{max} = 3$ , but the results were almost the same, as in the  $N_{max} = 2$  case.

The  $V^2$  occupation probabilities were taken either from a recent systematics of experimental data (refs. given in Ref. 3) or from BCS calculations.

The quasineutron energies were fitted indirectly to the level energies of the investigated odd-odd In nuclei. They were usually not far from the energies of the corresponding states of neighbouring odd Sn nuclei.

The  $I_0^p$ ,  $\chi_0^p$  and  $A_0^p$  parameters have been determined from the splitting of the  $\pi g_{9/2} \otimes 2_1^+$  multiplet of the neighbouring odd-even In nuclei by PTQM (particle truncated quadrupole phonon model)<sup>1,3)</sup> calculations.  $\chi^p$  is a parameter of the TQM quadrupole operator (see (6) in Ref. 13).  $A_0^p = 0$  is a reasonable value, taking into account that the phonon consists mainly of neutron excitations. The  $I_0^n$ ,  $A_0^n$ ,  $A_0^n$ ,  $v_D$  and  $v_S$  parameters were fitted to the energy spectra (and electro-

TABLE 2.

Parameters	<sup>116</sup> In		<sup>114</sup> In	<sup>112</sup> In	<sup>110</sup> In	<sup>108</sup> In	<sup>106</sup> In
	Set I	Set II					
Quadrupole phonon energies, MeV $\hbar\omega_2$	1.293		1.3	1.26	1.212	1.26	1.21
Occupation probabilities $V^2$ ( $\pi g_{5/2}$ )	0.91	0.944	0.87	0.87	1.0	1.0	1.0
$V^2$ ( $\nu d_{5/2}$ )	0.80	0.869	0.90	0.892	0.741	0.704	0.797
$V^2$ ( $\pi g_{7/2}$ )	0.45	0.399	0.78	0.674	0.594	0.359	0.203
$V^2$ ( $\nu s_{1/2}$ )	0.27	0.253	0.32	0.234	0.226	0.199	0.092
$V^2$ ( $\nu d_{3/2}$ )			0.20	0.145	0.103	0.047	0.051
Quasineutron energies, MeV $E$ ( $g_{1/2}$ )	0	0	0	0	0	0.23	0.45
$E$ ( $d_{5/2}$ )	1.25	1.33	0.91	0.81	0.20	0	0.35
$E$ ( $g_{7/2}$ )	0.866	0.99	0.93	0.36	0.59	0.06	0
$E$ ( $d_{3/2}$ )	0.15	0.22	0.37	0.32	0.75	1.43	1.4
Strength parameters of nucleon-core interaction, MeV $T_0^0$	1.1	1.0	1.0	1.9	1.0	0.9	1.0
$A_0^0$	0	0	0	0	0	0	0
$A_0^2$	0.1	0	0	0	0	0	0
$A_0^4$	0.7	0.5	0.7	0.8	0.8	0.5	0.3
$A_0^6$	0.2	1.1	0.8	0.8	2.5	1.9	2.4
$A_0^8$	0	0.15	0	0	0	0	0
Parameter of the TQM quadrupole operator, $\chi^p$	0	0	0	0	-0.4	-0.4	-0.4
Strength of residual int., MeV $\nu_D$	-0.4		-0.4	-0.4	-0.4	-0.5	-0.5
$\nu_S$	-0.1		-0.1	-0.1	-0.1	-0.08	-0.08
Effective charges, $e$	1.5	1.5	1.5	1.5	1.5	1.5	1.5
$e_{\nu p}^{p,p}$	0.5	0.5	0.5	0.5	0.5	0.5	0.5
$e_{\nu n}^{n,p}$	1.8	2.65	2.6	2.5	2.1	2.7	2.5
$e_{\nu n}^{n,n}$	0.45	0.5	0.5	0.5	0.5	0.5	0.5
Effective gyromagnetic ratios $g_1^p$	1	1	1	1	1	1	1
$g_1^n$	0	0	0	0	0	0	0
$g_2^n$	0	0	0	0	0	0	0
$g_1^p$	0	0	0	0	0	0	0
$g_1^n$	0	0	0	0	0	0	0
$g_2^n$	0	0	0	0	0	0	0
$g_1^p$	0	0	0	0	0	0	0
$g_1^n$	0	0	0	0	0	0	0
$g_2^n$	0	0	0	0	0	0	0
$g_1^p$	0	0	0	0	0	0	0
$g_1^n$	0	0	0	0	0	0	0
$g_2^n$	0	0	0	0	0	0	0
$g_1^p$	0	0	0	0	0	0	0
$g_1^n$	0	0	0	0	0	0	0
$g_2^n$	0	0	0	0	0	0	0
$g_1^p$	0	0	0	0	0	0	0
$g_1^n$	0	0	0	0	0	0	0
$g_2^n$	0	0	0	0	0	0	0
$g_1^p$	0	0	0	0	0	0	0
$g_1^n$	0	0	0	0	0	0	0
$g_2^n$	0	0	0	0	0	0	0
$g_1^p$	0	0	0	0	0	0	0
$g_1^n$	0	0	0	0	0	0	0
$g_2^n$	0	0	0	0	0	0	0
$g_1^p$	0	0	0	0	0	0	0
$g_1^n$	0	0	0	0	0	0	0
$g_2^n$	0	0	0	0	0	0	0
$g_1^p$	0	0	0	0	0	0	0
$g_1^n$	0	0	0	0	0	0	0
$g_2^n$	0	0	0	0	0	0	0
$g_1^p$	0	0	0	0	0	0	0
$g_1^n$	0	0	0	0	0	0	0
$g_2^n$	0	0	0	0	0	0	0
$g_1^p$	0	0	0	0	0	0	0
$g_1^n$	0	0	0	0	0	0	0
$g_2^n$	0	0	0	0	0	0	0
$g_1^p$	0	0	0	0	0	0	0
$g_1^n$	0	0	0	0	0	0	0
$g_2^n$	0	0	0	0	0	0	0
$g_1^p$	0	0	0	0	0	0	0
$g_1^n$	0	0	0	0	0	0	0
$g_2^n$	0	0	0	0	0	0	0
$g_1^p$	0	0	0	0	0	0	0
$g_1^n$	0	0	0	0	0	0	0
$g_2^n$	0	0	0	0	0	0	0
$g_1^p$	0	0	0	0	0	0	0
$g_1^n$	0	0	0	0	0	0	0
$g_2^n$	0	0	0	0	0	0	0
$g_1^p$	0	0	0	0	0	0	0
$g_1^n$	0	0	0	0	0	0	0
$g_2^n$	0	0	0	0	0	0	0
$g_1^p$	0	0	0	0	0	0	0
$g_1^n$	0	0	0	0	0	0	0
$g_2^n$	0	0	0	0	0	0	0
$g_1^p$	0	0	0	0	0	0	0
$g_1^n$	0	0	0	0	0	0	0
$g_2^n$	0	0	0	0	0	0	0
$g_1^p$	0	0	0	0	0	0	0
$g_1^n$	0	0	0	0	0	0	0
$g_2^n$	0	0	0	0	0	0	0
$g_1^p$	0	0	0	0	0	0	0
$g_1^n$	0	0	0	0	0	0	0
$g_2^n$	0	0	0	0	0	0	0
$g_1^p$	0	0	0	0	0	0	0
$g_1^n$	0	0	0	0	0	0	0
$g_2^n$	0	0	0	0	0	0	0
$g_1^p$	0	0	0	0	0	0	0
$g_1^n$	0	0	0	0	0	0	0
$g_2^n$	0	0	0	0	0	0	0
$g_1^p$	0	0	0	0	0	0	0
$g_1^n$	0	0	0	0	0	0	0
$g_2^n$	0	0	0	0	0	0	0
$g_1^p$	0	0	0	0	0	0	0
$g_1^n$	0	0	0	0	0	0	0
$g_2^n$	0	0	0	0	0	0	0
$g_1^p$	0	0	0	0	0	0	0
$g_1^n$	0	0	0	0	0	0	0
$g_2^n$	0	0	0	0	0	0	0
$g_1^p$	0	0	0	0	0	0	0
$g_1^n$	0	0	0	0	0	0	0
$g_2^n$	0	0	0	0	0	0	0
$g_1^p$	0	0	0	0	0	0	0
$g_1^n$	0	0	0	0	0	0	0
$g_2^n$	0	0	0	0	0	0	0
$g_1^p$	0	0	0	0	0	0	0
$g_1^n$	0	0	0	0	0	0	0
$g_2^n$	0	0	0	0	0	0	0
$g_1^p$	0	0	0	0	0	0	0
$g_1^n$	0	0	0	0	0	0	0
$g_2^n$	0	0	0	0	0	0	0
$g_1^p$	0	0	0	0	0	0	0
$g_1^n$	0	0	0	0	0	0	0
$g_2^n$	0	0	0	0	0	0	0
$g_1^p$	0	0	0	0	0	0	0
$g_1^n$	0	0	0	0	0	0	0
$g_2^n$	0	0	0	0	0	0	0
$g_1^p$	0	0	0	0	0	0	0
$g_1^n$	0	0	0	0	0	0	0
$g_2^n$	0	0	0	0	0	0	0
$g_1^p$	0	0	0	0	0	0	0
$g_1^n$	0	0	0	0	0	0	0
$g_2^n$	0	0	0	0	0	0	0
$g_1^p$	0	0	0	0	0	0	0
$g_1^n$	0	0	0	0	0	0	0
$g_2^n$	0	0	0	0	0	0	0
$g_1^p$	0	0	0	0	0	0	0
$g_1^n$	0	0	0	0	0	0	0
$g_2^n$	0	0	0	0	0	0	0
$g_1^p$	0	0	0	0	0	0	0
$g_1^n$	0	0	0	0	0	0	0
$g_2^n$	0	0	0	0	0	0	0
$g_1^p$	0	0	0	0	0	0	0
$g_1^n$	0	0	0	0	0	0	0
$g_2^n$	0	0	0	0	0	0	0
$g_1^p$	0	0	0	0	0	0	0
$g_1^n$	0	0	0	0	0	0	0
$g_2^n$	0	0	0	0	0	0	0
$g_1^p$	0	0	0	0	0	0	0
$g_1^n$	0	0	0	0	0	0	0
$g_2^n$	0	0	0	0	0	0	0
$g_1^p$	0	0	0	0	0	0	0
$g_1^n$	0	0	0	0	0	0	0
$g_2^n$	0	0	0	0	0	0	0
$g_1^p$	0	0	0	0	0	0	0
$g_1^n$	0	0	0	0	0	0	0
$g_2^n$	0	0	0	0	0	0	0
$g_1^p$	0	0	0	0	0	0	0
$g_1^n$	0	0	0	0	0	0	0
$g_2^n$	0	0	0	0	0	0	0
$g_1^p$	0	0	0	0	0	0	0
$g_1^n$	0	0	0	0	0	0	0
$g_2^n$	0	0	0	0	0	0	0
$g_1^p$	0	0	0	0	0	0	0
$g_1^n$	0	0	0	0	0	0	0
$g_2^n$	0	0	0	0	0	0	0
$g_1^p$	0	0	0	0	0	0	0
$g_1^n$	0	0	0	0	0	0	0
$g_2^n$	0	0	0	0	0	0	0
$g_1^p$	0	0	0	0	0	0	0
$g_1^n$	0	0	0	0	0	0	0
$g_2^n$	0	0	0	0	0	0	0
$g_1^p$	0	0	0	0	0	0	0
$g_1^n$	0	0					

magnetic properties) of the given odd-odd In nuclei. By the determination of the  $v_D$  and  $v_S$  parameters the results of the systematic works of Daehnick<sup>15)</sup> and Moinester et al.<sup>16)</sup> have been also taken into account.

The effective charges and gyromagnetic ratios were almost in all cases the commonly used standard values.

### 3.3. Results

The results of the IBFFM/OTQM calculations are presented and compared with experimental data in Figs. 5—7 (energy spectra) as well as in Tables 3—5

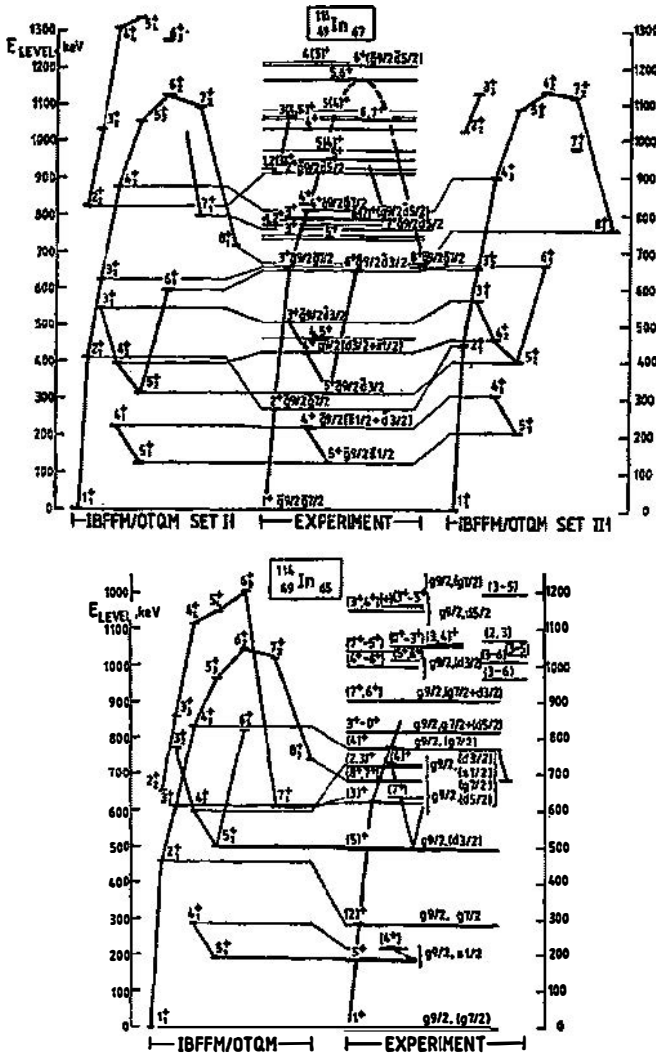


Fig. 5. Level schemes of low-lying positive parity states of <sup>116</sup>In (experimental<sup>7)</sup>, IBFFM/OTQM<sup>17)</sup> and <sup>114</sup>In (experimental<sup>1)</sup>, IBFFM/OTQM<sup>18)</sup>). Levels belonging to the same multiplet are connected.



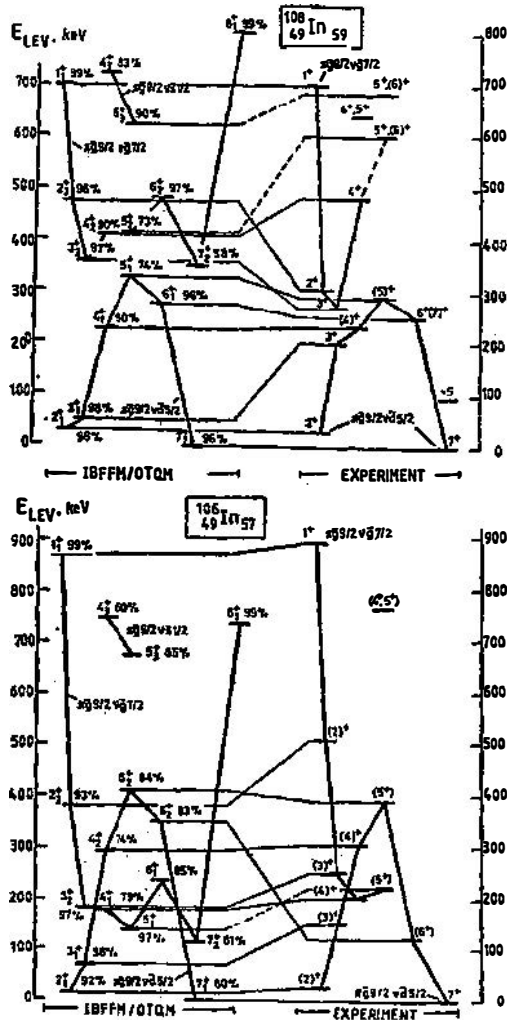


Fig. 7. IBFFM/OTQM and experimental level schemes of the low-lying positive parity states of  $^{108}\text{In}^{59}$  and  $^{106}\text{In}^{57}$ . After the spin and parity of the state purity is shown (in %), which characterizes the total strength of the given configuration in the wave function. States having the same main components are connected.

$2_2^+, 3_2^+, 4_4^+, 5_4^+, 6_3^+, 7_1^+$  with  $\pi\tilde{g}_{9/2}\nu\tilde{d}_{5/2}$  and  $3_3^+, 4_3^+, 5_2^+, 6_2^+$  with  $\pi\tilde{g}_{9/2}\nu\tilde{d}_{3/2}$  quasiparticles (Table 3), in accordance with the approximate classification of the parabolic rule. However, in the  $4_1^+, 5_1^+$  and  $4_3^+, 5_2^+$  states the components with  $\pi\tilde{g}_{9/2}\nu\tilde{s}_{1/2}$  and  $\pi\tilde{g}_{9/2}\nu\tilde{d}_{3/2}$  quasiparticles have comparable amplitudes.

The shape of *energy splitting* (Figs. 5—8) of the  $\pi\tilde{g}_{9/2}\nu\tilde{g}_{7/2}$  multiplet changes from an open-down parabola in  $^{116,114,112}\text{In}$  through a *W*-like pattern in  $^{108}\text{In}$  to an open-up (distorted) parabola in  $^{106}\text{In}$  (Fig. 8). As we have pointed out earlier the inversion is a consequence of the change in the occupation probability of the

TABLE 3.

$1_1^+$		$3_2^+$	
$\left(\frac{9}{2}, \frac{7}{2}\right)_{1,00}$	-0.806	$\left(\frac{9}{2}, \frac{5}{2}\right)_{2,12}$	-0.399
$\left(\frac{9}{2}, \frac{7}{2}\right)_{1,12}$	-0.259	$\left(\frac{9}{2}, \frac{5}{2}\right)_{3,00}$	-0.747
$\left(\frac{9}{2}, \frac{7}{2}\right)_{2,12}$	0.404	$\left(\frac{9}{2}, \frac{5}{2}\right)_{4,12}$	0.335
$\left(\frac{9}{2}, \frac{7}{2}\right)_{3,12}$	-0.273	$\left(\frac{9}{2}, \frac{5}{2}\right)_{5,12}$	-0.244
$2_1^+$		$3_3^+$	
$\left(\frac{9}{2}, \frac{5}{2}\right)_{2,00}$	0.242	$\left(\frac{9}{2}, \frac{3}{2}\right)_{3,00}$	0.787
$\left(\frac{9}{2}, \frac{7}{2}\right)_{1,12}$	-0.381	$\left(\frac{9}{2}, \frac{3}{2}\right)_{3,12}$	0.455
$\left(\frac{9}{2}, \frac{7}{2}\right)_{2,00}$	-0.718		
$\left(\frac{9}{2}, \frac{7}{2}\right)_{3,12}$	0.336		
$\left(\frac{9}{2}, \frac{7}{2}\right)_{4,12}$	-0.271		
$2_2^+$		$4_1^+$	
$\left(\frac{9}{2}, \frac{5}{2}\right)_{2,00}$	0.697	$\left(\frac{9}{2}, \frac{1}{2}\right)_{4,00}$	0.580
$\left(\frac{9}{2}, \frac{5}{2}\right)_{2,12}$	0.384	$\left(\frac{9}{2}, \frac{1}{2}\right)_{4,12}$	0.396
$\left(\frac{9}{2}, \frac{5}{2}\right)_{3,12}$	-0.406	$\left(\frac{9}{2}, \frac{3}{2}\right)_{4,00}$	0.488
$\left(\frac{9}{2}, \frac{7}{2}\right)_{2,00}$	0.225	$\left(\frac{9}{2}, \frac{3}{2}\right)_{4,12}$	0.336
		$\left(\frac{9}{2}, \frac{3}{2}\right)_{5,12}$	-0.228
$3_1^+$		$4_2^+$	
$\left(\frac{9}{2}, \frac{7}{2}\right)_{1,12}$	-0.258	$\left(\frac{9}{2}, \frac{7}{2}\right)_{2,12}$	-0.250
$\left(\frac{9}{2}, \frac{7}{2}\right)_{2,12}$	-0.315	$\left(\frac{9}{2}, \frac{7}{2}\right)_{3,12}$	-0.302
$\left(\frac{9}{2}, \frac{7}{2}\right)_{3,00}$	-0.747	$\left(\frac{9}{2}, \frac{7}{2}\right)_{4,00}$	-0.750
$\left(\frac{9}{2}, \frac{7}{2}\right)_{4,12}$	0.329	$\left(\frac{9}{2}, \frac{7}{2}\right)_{5,12}$	0.312
$\left(\frac{9}{2}, \frac{7}{2}\right)_{5,12}$	-0.275	$\left(\frac{9}{2}, \frac{7}{2}\right)_{6,12}$	-0.259
$4_3^+$		$6_2^+$	
$\left(\frac{9}{2}, \frac{1}{2}\right)_{4,00}$	-0.517	$\left(\frac{9}{2}, \frac{3}{2}\right)_{5,12}$	-0.304
$\left(\frac{9}{2}, \frac{1}{2}\right)_{4,12}$	-0.313	$\left(\frac{9}{2}, \frac{3}{2}\right)_{6,00}$	-0.608

TABLE 3 continued.

$\left(\frac{9}{2}, \frac{3}{2}\right)_{4,00}$	0.593	$\left(\frac{9}{2}, \frac{3}{2}\right)_{6,12}$	-0.307
$\left(\frac{9}{2}, \frac{3}{2}\right)_{4,12}$	0.331	$\left(\frac{9}{2}, \frac{7}{2}\right)_{6,00}$	0.480
$5^{\dagger}$		$7^{\dagger}$	
$\left(\frac{9}{2}, \frac{1}{2}\right)_{5,00}$	-0.609	$\left(\frac{9}{2}, \frac{5}{2}\right)_{7,00}$	-0.681
$\left(\frac{9}{2}, \frac{1}{2}\right)_{5,12}$	-0.433	$\left(\frac{9}{2}, \frac{5}{2}\right)_{7,12}$	-0.554
$\left(\frac{9}{2}, \frac{3}{2}\right)_{5,00}$	0.458	$\left(\frac{9}{2}, \frac{7}{2}\right)_{7,00}$	-0.317
$\left(\frac{9}{2}, \frac{3}{2}\right)_{5,12}$	0.334		
$5^{\ddagger}$		$7^{\ddagger}$	
$\left(\frac{9}{2}, \frac{1}{2}\right)_{5,00}$	-0.460	$\left(\frac{9}{2}, \frac{5}{2}\right)_{7,00}$	0.312
$\left(\frac{9}{2}, \frac{1}{2}\right)_{5,12}$	-0.253	$\left(\frac{9}{2}, \frac{5}{2}\right)_{7,12}$	0.251
$\left(\frac{9}{2}, \frac{3}{2}\right)_{4,12}$	-0.302	$\left(\frac{9}{2}, \frac{7}{2}\right)_{7,00}$	-0.718
$\left(\frac{9}{2}, \frac{3}{2}\right)_{5,00}$	-0.607	$\left(\frac{9}{2}, \frac{7}{2}\right)_{7,12}$	-0.403
$\left(\frac{9}{2}, \frac{3}{2}\right)_{5,12}$	-0.290	$\left(\frac{9}{2}, \frac{7}{2}\right)_{8,12}$	0.237
$5^{\ddagger}$		$8^{\dagger}$	
$\left(\frac{9}{2}, \frac{7}{2}\right)_{3,12}$	-0.260	$\left(\frac{9}{2}, \frac{7}{2}\right)_{8,00}$	-0.776
$\left(\frac{9}{2}, \frac{7}{2}\right)_{4,12}$	-0.295	$\left(\frac{9}{2}, \frac{7}{2}\right)_{8,12}$	-0.552
$\left(\frac{9}{2}, \frac{7}{2}\right)_{5,00}$	-0.787		
$\left(\frac{9}{2}, \frac{7}{2}\right)_{6,12}$	0.303		
$6^{\dagger}$			
$\left(\frac{9}{2}, \frac{3}{2}\right)_{6,00}$	0.471		
$\left(\frac{9}{2}, \frac{3}{2}\right)_{6,12}$	0.263		
$\left(\frac{9}{2}, \frac{7}{2}\right)_{6,00}$	0.645		
$\left(\frac{9}{2}, \frac{7}{2}\right)_{6,12}$	0.233		
$\left(\frac{9}{2}, \frac{7}{2}\right)_{7,12}$	-0.226		

Wave functions of low-lying positive parity states of  $^{112}\text{In}$  calculated in IBFFM/OTQM<sup>2)</sup>. For a given  $\gamma^{\pi}$  state the  $(j_{\beta}, j_{\alpha}) I, NR$  values are shown. Only amplitudes larger than 5% are listed.

TABLE 4.

Electro-magnetic moments	$^{116}\text{In}^{17*}$		$^{114}\text{In}^{18*}$		$^{112}\text{In}^{20*}$		$^{110}\text{In}^{42*}$		$^{108}\text{In}^{52*}$		$^{106}\text{In}^{62*}$
	$J^\pi$ $T_{1/2}$	$1^\dagger$ $5^\dagger$ min	$1^\dagger$ $5^\dagger$ s	$1^\dagger$ $5^\dagger$ d	$1^\dagger$ $4^\dagger$ min	$7^\dagger$ $0.69$ $\mu\text{s}$	$7^\dagger$ $4.9$ h	$2^\dagger$ $69.1$ min	$7^\dagger$ $58.0$ min	$2^\dagger$ $3.96$ min	$7^\dagger$ $6.2$ min
$\mu_{exp}$	2.7863(10)	4.235(15)	2.815 (11)	4.653(5)	2.82(3)	4.056(36)	4.713(8)	4.365(4)	4.561(3)	4.935(5)	4.916(7)
$\mu_{emp}^{**}$	3.04	4.53	3.04	4.61	3.07	4.44			4.73 4.291	5.12	4.975 4.83
Set I $\mu_{IBFFM}$	2.75	4.51		4.55		4.54	4.84	4.43	4.41	4.895	4.60
Set II $\mu_{theor}^{19}$	2.79	4.44	2.87	5.028	2.82		4.876	4.175	5.40		4.415
$\mu_{theor}^{20}$	2.842	4.92	2.837	4.45	2.84						
$\mu_{theor}^{21}$	2.93	4.55	2.93								
$Q_{exp}$	0.09(2)	0.802(12)		0.739(12)	0.093	0.714(10)	1.000(22)	0.37	1.005(7)	0.467(14)	0.972(61)
$Q_{emp}^{**}$	0.11(1)	0.82	0.178	0.80	0.17	1.11	1.15		1.15	0.53	1.24
Set I $Q_{IBFFM}$	0.136	0.66									
Set II $Q_{theor}^{19}$	0.145	0.62	0.15	0.74	0.14	0.84	0.93	0.41	1.00	0.466	0.96
$Q_{theor}^{20}$	0.056		0.055		0.102		0.60	0.24			
$Q_{theor}^{21}$	0.104										

Magnetic dipole ( $\mu$  in  $\mu_N$ ) and electric quadrupole ( $Q$  in eb) moments of some  $^{116,114,112,110,108,106}\text{In}$  states.

\* Sources of experimental and empirical data are detailed in these publications.

\*\* The empirical values were obtained from experimental moments of the neighbouring single-odd In, Sn and Cd nuclei on the basis of simple additivity relations.

TABLE 5.

States				$E_\gamma$ (keV)	$I_{\gamma}^{rel}/E_{\gamma}^3$		Type		IBFFM
$E_i$ (keV)	$J_i^{\pi}$	$E_f$ (keV)	$J_f^{\pi}$		Exp. <sup>2)</sup>	IBFFM	Ref. 2	Ref. 22	
206.72	$2_1^+$	0.01	$1_1^+$	206.75		M1		M1 + 0.084% E2	
456.45	$3_1^+$	206.72	$2_1^+$	249.68		M1		M1 + 0.079% E2	
562.79	$5_2^+$	162.90	$(5_1)^+$	399.88	52(3)	M1, E2		M1 + 0.004% E2	
		156.61	$4_1^+$	406.18	100	M1, E2		M1 + 0.61% E2	
592.10	$4_2^+$	456.45	$3_1^+$	135.64	100	M1	M1 + 0.01(20)% E2	M1 + 0.022% E2	
594.87	$2_2^+$	162.90	$(5_1)^+$	429.17	0.3(1)			M1 + 0.018% E2	
		456.45	$3_1^+$	138.37	69(8)			M1 + 0.003% E2	
		206.72	$2_1^+$	388.20	100	M1, E2	M1 + 0.25(50)% E2	M1 + 0.051% E2	
790.28	$(7_2^+, 8)^+$	0.0	$1_1^+$	594.85	83(4)	M1, (E2)	M1 + 1.0(6)% E2	M1 + 0.97% E2	
		670.24	$8_1^+, 7^+(6)^+$	120.01	100			M1 + 0.024% E2	
		350.81	$7_1^+$	439.49	20(4)	M1, E2		M1 + 0.32% E2	
795.27	$5_3^+$	592.10	$4_2^+$	203.17		M1	M1 + 0.01(22)% E2	M1 + 0.054% E2	
833.10	$6_1^+$	562.79	$5_2^+$	270.22	43(10)			M1 + 0.27% E2	
		350.81	$7_1^+$	482.39	100	M1, E2		M1 + 0.10% E2	
		162.90	$(5_1)^+$	670.19	4(1)	M1		M1 + 4.9% E2	
883.79	$3_2^+$	594.87	$2_2^+$	288.92	100	M1	M1 + 0.25(30)% E2	M1 + 0.13% E2	
		592.10	$4_2^+$	291.5	4(2)			M1 + 0.32% E2	
		456.43	$3_1^+$	427.39	3(1)			M1 + 1.1% E2	
		156.61	$4_1^+$	727.25	5(1)			M1 + 0.003% E2	

Transitions within low-lying  $^{112}\text{In}$  states.

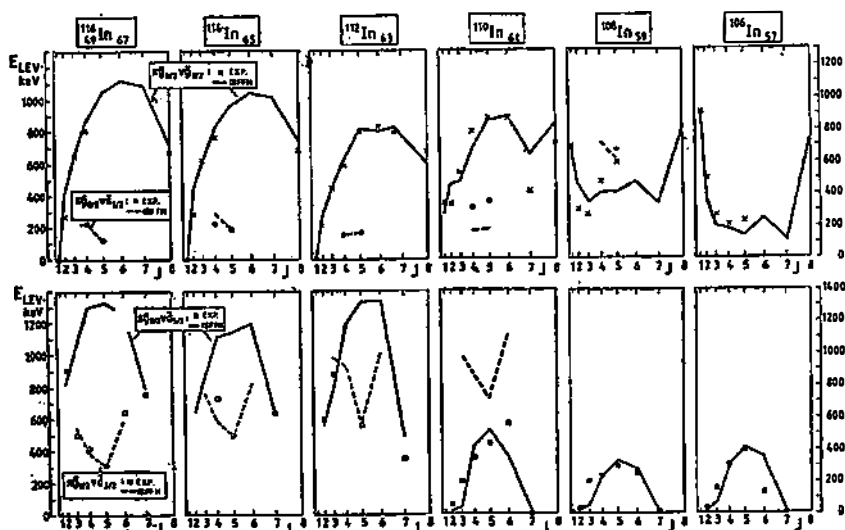


Fig. 8. Energy splitting of the  $\pi g_{7/2}\nu g_{7/2}$ ,  $\pi g_{9/2}\nu s_{1/2}$ ,  $\pi g_{9/2}\nu d_{5/2}$  and  $\pi g_{9/2}\nu d_{3/2}$  multiplets in odd-odd  $^{116-106}\text{In}$  nuclei as a function of  $J(J+1)$  where  $J$  is the spin of the state.

$g_{7/2}$  neutron orbit; the  $g_{7/2}$  quasineutron is hole like in  $^{116}_{49}\text{In}_{67}$ ,  $^{114}_{49}\text{In}_{65}$ ,  $^{112}_{45}\text{In}_{63}$  and particle-like in  $^{106}_{49}\text{In}_{57}$ .

The  $W$ -like distortion of the parabola is caused by the neutron-phonon exchange interaction. By fine tuning of the phonon-neutron quasiparticle dynamical and exchange interactions the general features of the form-change can be described. The dynamical interaction is strong near  $V_p^2 = 0$  or 1, and weak near  $V_p^2 = 0.5$ ; while the exchange interaction plays an important role only around the Fermi level ( $V_p^2 \approx 0.5$ ). The increased strength of the exchange interaction points out the increased role of the Pauli principle in  $^{110,108}\text{In}$  (and partly in  $^{106}\text{In}$ ). A similar change of pattern was observed at the  $\pi \tilde{g}_{7/2}\nu \tilde{h}_{11/2}$  multiplet of  $^{134}\text{Cs}^{23}$ , too.

The splitting of the  $\pi \tilde{g}_{9/2}\nu \tilde{s}_{1/2}$  doublet is reproduced well in  $^{116,114,112,110}\text{In}$ :  $E(4_1^+) > E(5_1^+)$  in  $^{116,114}\text{In}$  and  $E(4_1^+) < E(5_1^+)$  in  $^{112,110}\text{In}$ . The  $4_1^+$ ,  $5_1^+$  states of  $^{116,114}\text{In}$  and the  $5_1^+$  states of  $^{110}\text{In}$  are rather pure, while the others are strongly mixed.

The splitting of the  $\pi \tilde{g}_{9/2}\nu \tilde{d}_{5/2}$  multiplet has an open-down parabolic shape. The parabola is sinking down with decreasing neutron number. Both features have been described reasonably well by the calculations.

The energies of the members of  $\pi \tilde{g}_{9/2}\nu \tilde{d}_{3/2}$  multiplet have been reproduced well in  $^{116}\text{In}$ , in the lighter odd-odd In nuclei the experimental data are incomplete.

The sign of the  $\mu_{exp}$  and  $Q_{exp}$  moments (Table 4 and Fig. 9) was properly reproduced by the IBFFM/OTQM calculations. The  $\mu_{exp}$  and  $\mu_{IBFFM}$  values agree within a few percents. The deviations among the  $Q_{exp}$  and  $Q_{IBFFM}$  values are larger, but even these agree within  $\lesssim 50\%$ . The IBFFM calculations show, that the contribution of the collective electromagnetic operator is relatively small to the magnetic dipole moments, and is significant to the  $Q$  values. This can explain, why the simple additivity relation predicts the magnetic moments correctly.

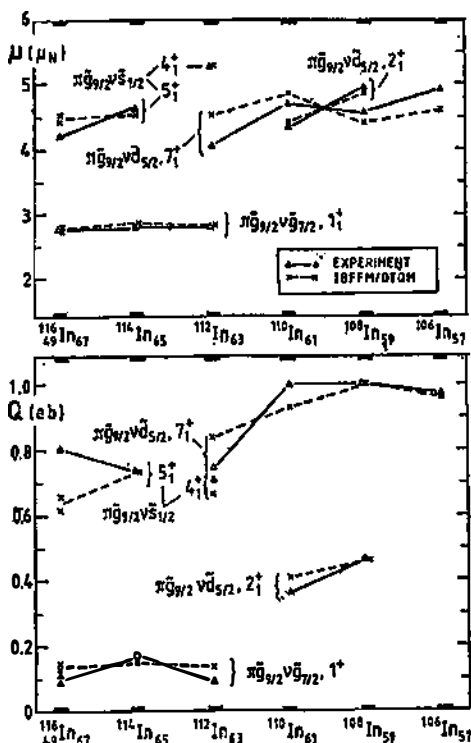


Fig. 9. Experimental and IBFFM/OTQM electromagnetic moments of odd-odd  $^{116-106}\text{In}$  nuclei. Here  $\circ$  indicates empirical result which was calculated from the experimental magnetic moments of the neighbouring single-odd nuclei by the use of additivity relation.

In Table 5 we present the *reduced transition probabilities* and  $\gamma$ -mixing ratios of  $M1 + E2$  transitions between the low-lying states of  $^{112}\text{In}$ .

In the majority of cases the  $\gamma$ -branching ratios from the low-lying positive parity states of  $^{116,114,112,110,108,106}\text{In}$  were reproduced by the IBFFM/OTQM calculations within a factor of about 7. The IBFFM/OTQM  $\gamma$ -mixing ratios are usually very small and agree with the existing experimental data within error limits.

Prior to the above mentioned IBFFM/OTQM calculations detailed theoretical analysis was not performed on the positive parity state of  $^{112,110,108,106}\text{In}$ . The level properties of  $^{116}\text{In}$  and  $^{114}\text{In}$  were calculated in the framework of the hole-quasiparticle model by Rabenstein et al.<sup>24,25)</sup> using quadrupole-quadrupole residual p-n interaction and by Van Gunsteren<sup>20)</sup> who has used renormalized Schiffer interaction. The energy splittings of the p-n multiplets of  $^{116}\text{In}$  were described by Alexeev et al.<sup>7)</sup> using Wigner and singlet p-n residual interactions. The present IBFFM/OTQM calculations give a more complete description of the positive parity states of  $^{116}\text{In}$  and  $^{114}\text{In}$ . The  $\pi\tilde{g}_{9/2}\tilde{\nu}h_{11/2}$  negative parity states of the odd-odd In nuclei have been described in detail in the recent works of Van Maldeghem et al.<sup>19)</sup> and Alexeev et al.<sup>26)</sup>

## Acknowledgements

We are indebted to all co-authors of Refs. 1—6, 14 for fruitful collaboration. The financial support of the Hungarian National Scientific Research Foundation (OTKA) is gratefully acknowledged. One of us (Zs. D.) thanks International Centre for Theoretical Physics (Trieste) for providing computational facilities.

## References

- 1) J. Timár, T. Fényes, T. Kibédi, A. Passoja, M. Luontama, W. Trzaska and V. Paar, Nucl. Phys. **A455** (1986) 477;
- 2) T. Kibédi, Zs. Dombrádi, T. Fényes, A. Krasznahorkay, J. Timár, Z. Gácsi, A. Passoja, V. Paar and D. Vretenar, Phys. Rev. **C37** (1988) 2391;
- 3) A. Krasznahorkay, T. Fényes, J. Timár, T. Kibédi, A. Passoja, R. Julin and J. Kumpulainen, Nucl. Phys. **A473** (1987) 471;
- 4) A. Krasznahorkay, Zs. Dombrádi, J. Timár, Z. Gácsi, T. Kibédi, A. Passoja, R. Julin, J. Kumpulainen, S. Brant and V. Paar, ATOMKI Preprint P1-1989, 1989, Debrecen; Nucl. Phys. A in press;
- 5) A. Krasznahorkay, Zs. Dombrádi, J. Timár, T. Fényes, J. Gulyás, J. Kumpulainen and E. Verho, Nucl. Phys. A in press;
- 6) J. Gulyás, Zs. Dombrádi, T. Fényes, J. Timár, A. Passoja, J. Kumpulainen and R. Julin, ATOMKI Preprint 3-1989 P, 1989, Debrecen, to be published in Nucl. Phys.;
- 7) V. L. Alexeev, B. A. Emelianov, D. M. Kaminker, Yu. L. Khazov, I. A. Kondurov, Yu. E. Loginov, V. L. Rumiantsev, S. L. Sakharov and A. I. Smirnov, Nucl. Phys. **A262** (1976) 19;
- 8) V. Paar, Nucl. Phys. **A331** (1979) 16;
- 9) T. Fényes, in *In-Beam Nuclear Spectroscopy*, ed. Zs. Dombrádi and T. Fényes, Budapest Akad. Kiado, 1984, vol. 1, p. 67;
- 10) W. B. Walters, in *In-Beam Nuclear Spectroscopy*, ed. Zs. Dombrádi and T. Fényes, Budapest Akad. Kiado, 1984, vol. 1, p. 251;
- 11) V. Paar, in *In-Beam Nuclear Spectroscopy*, ed. Zs. Dombrádi and T. Fényes, Budapest Akad. Kiado, 1984, vol. 2, p. 675;
- 12) A. B. Balantekin and V. Paar, Phys. Lett. **169B** (1986) 9;
- 13) V. Paar, S. Brant, L. F. Canto, G. Leander, and M. Vouk, Nucl. Phys. **A378** (1982) 41;
- 14) S. Brant, V. Paar and D. Vretenar, IKP Jülich, 1985, unpublished;
- 15) W. V. Daehnick, Phys. Rep. **96** (1983) 317;
- 16) M. Moinester, J. P. Schiffer and V. P. Alford, Phys. Rev. **179** (1969) 984;
- 17) T. Fényes and Zs. Dombrádi, ATOMKI Preprint 6-1988 P, 1988, Debrecen; Acta Phys. Hung. **65** (1989) 292;
- 18) Zs. Dombrádi and T. Fényes, ATOMKI Ann. Rep. 1988, p. 22, Debrecen;
- 19) J. Van Maldeghem, K. Heyde and J. Sau, Phys. Rev. **C32** (1985) 1067;
- 20) W. F. Van Gunsteren, Nucl. Phys. **A265** (1976) 263;
- 21) A. Winnacker, unpublished;
- 22) T. Kohno, M. Adachi and H. Taketani, Nucl. Phys. **A398** (1983) 493;
- 23) S. Brant, V. Paar, D. Vretenar, G. Alaga, H. Seyfarth, O. Schult and M. Bogdanović, Phys. Lett. **B195** (1987) 111;
- 24) D. Rabenstein, D. Harrach, H. Vonach, G. G. Dussel and R. P. I. Perazzo, Nucl. Phys. **A197** (1972) 129;
- 25) D. Rabenstein and D. Harrach, Nucl. Phys. **A242** (1975) 189;
- 26) V. L. Alexeev, S. A. Artamonov, V. I. Isakov and S. L. Sakharov, Proc of 6th Int. Symp. on capture  $\gamma$ -ray spectroscopy, Leuven, 1987, ed. P. Van Assche and K. Abrahams (Inst. of Phys. Conf. Series 88, Bristol, 1988), p. 516.

STRUKTURA NEPARNO-NEPARNIH In JEZGRI

TIBOR FÉNYES, ZSOLT DOMBRÁDI, ATTILA KRASZNAHORKAY, JÁNOS GULYÁS, JÁNOS TIMÁR, TIBOR KIÉDI i VLADIMIR PAAR\*

*Institute of Nuclear Research of the Hung. Acad. Sci. 4001 Debrecen, Hungary*

*\* Prirodoslovno-matematički fakultet, Univ. of Zagreb, Zagreb, Yugoslavia*

UDK. 539.144

Originalni znanstveni rad

Proučavana je struktura neparno-neparnih jezgri indija složenim metodama  $\gamma$  i elektronske spektroskopije, koristeći reakcije  $(p, n\gamma)$  i  $(\alpha, n\gamma)$ . Energetski spektri i elektromagn. prelazi su izračunati u okviru IBFFM-a.